Turbulence Characteristics of Flow over a Block Ramp

Z Ahmad[1], Himanshu Sharma[2], Bernhard Westrich[3]

*[1, 2]Department of Civil Engineering, Indian Institute of Technology Roorkee, Roorkee, Uttarakhand-247667, India
[3]Institute of Hydraulics Engineering (IWS), University of Stuttgart, Germany

*[1]zulfifce@iitr.ernet.in; [2]smile4anshu@gmail.com; [3]bernhard.westrich@iws.uni-stuttgart.de

***Abstract*- Block ramps are structures consisting of boulders on steep slope and used for the stabilization of streams by dissipation of energy of flow by means of generating excessive turbulence. This paper deals with experimental study of turbulence over a block ramp. Three-dimensional velocities were measured by acoustic Doppler velocity meter at a constant depth along the block ramp in the developing flow zone. Spiky velocity data were removed using computer code developed in this study for four filtering methods. Out of other filtering methods, the velocity correlation method was found more effective. Spatial variation of turbulence intensities, Reynolds stress, turbulent kinetic energy and skewness coefficients of velocity fluctuations along the length of block ramp were studied. The longitudinal turbulence intensity increases along the ramp length, while the vertical turbulence intensity decreases. Reynolds stresses and turbulent kinetic energy increase along the block rampas a result of development of boundary layer. Skewness coefficients of the longitudinal and transverse velocity components were observed to be uncorrelated with the block ramp length whereas skewness coefficient of vertical velocity component was observed to vary linearly with the length of block ramp.**

Keywords- Turbulence; Block Ramps; Spikes; Turbulent Intensities; Reynolds Stress; Turbulent Kinetic Energy

I. INTRODUCTION

Turbulence is an inherent property of flow and can be defined as spatially and temporally varying flow phenomenon, which can be predicted by use of statistical parameters. Various studies have been conducted on turbulent flow in open channel (Blinco and Partheniades, 1970; Grass, 1971; Nezu and Rodi, 1986; Wang et al.1993; Carollo et al. 2005 etc.). Grass (1971) studied the structural features of turbulence on smooth, transitionally rough and rough beds and extended the concept of bursting events in boundary layer given by Kline et al. (1967). Nezu and Rodi (1986) studied the turbulence by using Laser Doppler Anemometer (LDA) and developed equations for the vertical distribution of turbulent intensities for smooth bed. They observed that the turbulent intensities decrease exponentially from bed to water surface. Chen and Chiew (2003) studied the effect of sudden roughness change on turbulence.

Block ramps can be defined as structures consisting of boulders on steep slope or stepped chute which can be used to dissipate energy of flow by means of generating excessive turbulence. Flow skims off over the boulders and causes the dissipation of energy by forming high amount of eddies and turbulence. Previous studies on block mainly deal with factors affecting energy dissipation, however, no worth notice was given on the aspect of distribution of various turbulence parameters on block ramps which may affect the process of energy dissipation(Pagliara and Chiavaccini, 2006;Pagliara et al. 2008;PagliaraandLotti, 2009; Ahmad et al., 2009; Ghare et al. 2010, etc.). This paper deals with spatial variation of turbulence parameters of flow over block ramps with use of measured three-dimensional velocities by Acoustic Doppler Velocimeter (ADV).

II. REVIEW OF FILTERING METHODS

The ADV is based on Doppler back-scattered measuring system which measures the velocities after receiving the transmitted waves Doppler-shifted. Thus errors related to the Doppler back-scattered measuring system are automatically possessed by ADV. The most common errors in ADV measuring system are Doppler noise which is by virtue of turbulence of flow, amount of particles in flow, sensor geometry, etc. and aliasing of acoustic signals. These errors generate some spurious and uncorrelated velocity data in time series of measurements called as spikes. Various methods are given in literature to filter out the spiked data, however the most commonly four methods are described here.

A. Maximum and Minimum Threshold Method

This method assumes that velocity data follow the Gaussian distribution. The universal thresholding parameter, λ, is used to define maximum and minimum range of data. The velocity data are considered to be corrupted or invalid if they lie outside the range established by (Cea et al. 2007):

$$u_{\min} = \overline{u} - \lambda\sigma_u ; \quad u_{\max} = \overline{u} + \lambda\sigma_u \tag{1a-b}$$

where, u_{min} and u_{max} are minimum and maximum velocity threshold in x- direction, respectively,$\bar{u}$ = time-averaged velocity in x- direction, λ = universal threshold =$\sqrt{2\ln(N)}$, σ_u= standard deviation of velocity in x- direction, N = number of data-points. Similar expressions can be used for velocity threshold of other two velocity components.

B. Acceleration Threshold Method

Acceleration or deceleration in the flow is proportional to acceleration due to gravity i.e., $a_i = \lambda_a g$. Here, a_i = acceleration at 'i^{th}' time interval; λ_a = proportionality constant; g = acceleration due to gravity. Goring and Nikora (2002) proposed λ_a = 1-1.5 by conducting a large number of experiments. Cea et al. (2007) divided λ_a into components of x, y and z-directions in the following way:

$$\lambda_{ax} = \lambda\sigma_{ax}/g \; ; \; \lambda_{ay} = \lambda\sigma_{ay}/g; \; \lambda_{az} = \lambda\sigma_{az}/g \tag{2a-c}$$

Here, σ_{ax}, σ_{ay}, σ_{az} are the standard deviations of acceleration components in x, y and z-directions, respectively. Values of these components were observed to be more or less near to λ_a proposed by Goring and Nikora (2002). This method despikes the data in two phases, out of which first is assigned for deceleration phase and second for acceleration phase of flow. Firstly acceleration is calculated by back-difference method for a given time interval, say Δt, by

$$a_i = \left(u_i - u_{i-1}\right)/\Delta t \tag{3}$$

Then those points are removed which surpass the threshold limits given by $a_i < -\lambda_a g$ and $u_i < \bar{u} - k_\sigma \sigma_u$ (k_σ is a proportionality constant and≈1.5).Since by removing or replacing the data some statistical parameters are changed, thus for second phase of positive acceleration new standard deviation, σ_u is calculated and again data are replaced or removed if acceleration surpasses the threshold limits given by $a_i > \lambda_a g$ and $u_i > \bar{u} + k_\sigma \sigma_u$.

C. Phase-Space Threshold Method

This method utilizes the Poincare map to distinguish unbiased data with spikes by plotting variable with its derivatives (Goring and Nikora, 2002). Firstly by using central difference method, the first and second derivatives of velocity are calculated as

$$\Delta u_i = \left(u_{i+1} - u_{i-1}\right)/2 \; ; \quad \Delta^2 u_i = \Delta u_{i+1} - \Delta u_{i-1}/2 \tag{4a-b}$$

The standard deviations of all the three variables i.e. u, Δu and $\Delta^2 u$ are calculated and labeled as σ_u, $\sigma_{\Delta u}$ and $\sigma_{\Delta^2 u}$. Their expected maximum values are fixed by

$$u_{\max} = \lambda\sigma_u \; ; \; \Delta u_{\max} = \lambda\sigma_{\Delta u} \; ; \; \Delta^2 u_{\max} = \lambda\sigma_{\Delta^2 u} \tag{5a-c}$$

The data are plotted for Δu_i versus u_i, $\Delta^2 u_i$ versus Δu_i and $\Delta^2 u_i$ versus u_i. The ellipsoid formed from the data of Δu_i versus u_i, and $\Delta^2 u_i$ versus Δu_i, is symmetrical with respect to principal axes with their major and minor axes coinciding with the principal axes, however in case of ellipsoid formed from $\Delta^2 u_i$ versus u_i axes are inclined at certain angle, θ

$$\theta = \tan^{-1}\left(\sum u_i \Delta^2 u_i \Big/ \sum u_i^2\right) \tag{6}$$

The major and minor axes of ellipsoid of Δu_i and u_i are given as $\lambda\sigma_u$ and $\lambda\sigma_{\Delta u}$, respectively. Data lying outside the periphery of the ellipsoid are curtailed off and recalculation of the standard deviations for u, Δu and $\Delta^2 u$are carried out. The data are curtailed off if they lie outside the periphery of ellipsoid formed by $\Delta^2 u_i$ and Δu_i, whose major and minor axes are given by $\lambda\sigma_{\Delta u}$ and $\lambda\sigma_{\Delta^2 u}$. The statistical parameters are calculated again for u, Δu and $\Delta^2 u$. For ellipsoid formed by $\Delta^2 u_i$ and u_i, the major and minor axes, a and b respectively, are given by

$$(\lambda\sigma_u)^2 = a^2 \cos^2\theta + b^2 \sin^2\theta \; ; \quad \left(\lambda\sigma_{\Delta^2 u}\right)^2 = a^2 \sin^2\theta + b^2 \cos^2\theta \tag{7a-b}$$

The ellipsoid with major and minor axes as a and b, respectively is plotted and the data are removed which lie outside of the ellipsoid boundary. Wahl (2003) improved the method by using median and median of the absolute deviations as location and scale estimator instead of standard deviation and universal threshold parameter, λ.

D. Velocity Correlation Method

In this method, the fluctuations of velocity components u' and v' are plotted against each other i.e., u'-v', which forms an ellipse. The data which fall outside of the ellipse periphery are considered as spikes. Firstly filtering is done and cleaned record is used to plot mean flow statistics. This method is advantageous where flow is highly turbulent with large concentration of spikes and where replacing algorithm can give rise to more spikes. Following formula are used to obtain the values of major and minor axes of ellipse i.e., a and b, respectively, and also the angle of rotation with principal axes θ.

$$a^2 = \frac{(\lambda\sigma_u \cos\theta)^2 - (\lambda\sigma_v \sin\theta)^2}{\cos^2\theta - \sin^2\theta};\ b^2 = \frac{(\lambda\sigma_v \cos\theta)^2 - (\lambda\sigma_u \sin\theta)^2}{\cos^2\theta - \sin^2\theta};\ m = tan\theta = \frac{\overline{u'v'}}{\overline{u'^2}} \quad (8, 9, 10)$$

Similar expressions are used for the u'-w' and v'-w' velocity planes.

III. EXPERIMENTAL WORKS

The experiment was performed in a rectangular channel of length 7.5 m, width 1.5 m and depth 1.0 m at Institute of Hydraulics Engineering (IWS), University of Stuttgart, Germany. Fig. 1 shows photograph of the experimental set up. The bed slope of the channel was 3.5%. Crushed boulders of size varying from 7-25 cm were placed on the bed of the channel in a thickness of 27 cm (Fig. 2). A tank was connected to the channel at its head and another tank was provided at tail of the channel. Water was supplied to the channel through a supply line in which a magnetic flow meter was fit for the measurement of discharge. Experiments were performed for the maximum discharge of the system equal to 0.462 m^3/s. The water surface profile in the channel was measured using point gauge of accuracy ±0.1 mm. The three dimensional velocities were measured at different longitudinal distances from the head of the channel at a depth of 10.5 cm and mid of the channel using ADV.

Fig. 1 Experimental setup of block ramp

Fig. 2 Boulder bed of block ramp

IV. ANALYSIS OF DATA

A. Water Surface Profile

Water surface profile measured for maximum discharge, Q=0.462 m^3/s at the mid of the channel is depicted in Fig.3. The profile can be divided into three regions, i.e., gradually varied flow (GVF) from x= 0 to 220 cm; uniform flow from x = 220 to 650 cm and rapidly varied flow (RVF) near the end of the channel having a vertical drop. The depth of flow in the uniform flow was 15.5 cm.

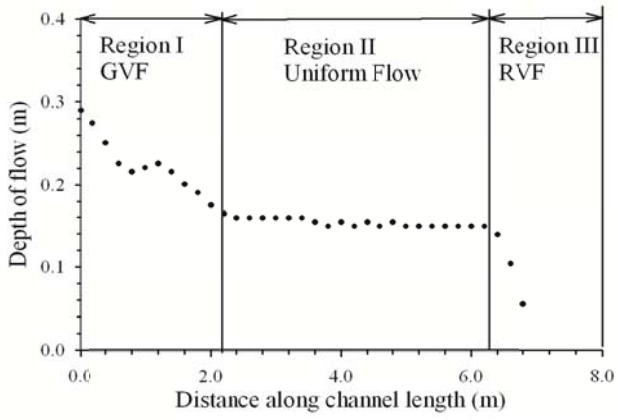

Fig. 3 Water surface profile over the block ramp

B. Filtering of Observed Velocity Data

The three dimensional velocities measured at various points along the length of channel from x=8 to 198 cm at a constant depth of 10.5 cm from the tip of the boulders. Signal-Noise Ratio (SNR) values of measured data were around 44 dB, which is

higher than 10 dB required for the elimination of data by SNR criterion. Correlation coefficient (COR) of measured data was 30%-65%, which is lower than the 70%, the minimum COR prescribed by the ADV manufacturer.

A computer code was developed to filter the observed velocity data using four methods, discussed above. The Maximum and minimum threshold filter filtered out very few numbers of data as spikes even though a number of spikes were present in the data. Filtering the measured velocities by acceleration threshold and phase-space threshold methods did not produce fertile results as these methods do not recognized any spikes in the velocity data. Acceleration threshold method and phase space threshold method are applicable to those flow conditions, whose spikes are so much deviated from time-averaged velocity that a few amounts of these can enhance standard deviation of velocity by a large extent. Out of all the above discussed methods, velocity correlation method was observed to be most suitable. The observed velocity data shown in Fig. 4(a) were first filtered with *u*' - *v*' ellipsoid, the resulting velocity data are shown in Fig. 4b and 4c in *u*' - *v*' and *v*' - *w*' profiles, respectively. The filtered data in *u*' - *v*' ellipsoid were then filtered by *v*' - *w*' ellipsoid. The filtered data are shown in Fig. 4d and 4e in *v*' - *w*' and *w*'- *u*' profiles, respectively. The remaining data were then filtered with *w*'- *u*' ellipsoid and the final filtered data are shown in Fig. 4f. These figures depict that velocity data filtered with one velocity correlation profile have spiky data. Therefore, for the removal of the spikes, the data should be filtered with all the three velocity correlation profiles. Unfiltered and filtered *u*, *v* and *w* are shown in Fig. 5, which clearly indicates that the velocity correlation method effectively removes the spikes from the velocity data. This method detected around 22% data as spikes in the observations, which were around 13 times more than the amount of spikes detected by maximum and minimum threshold method.

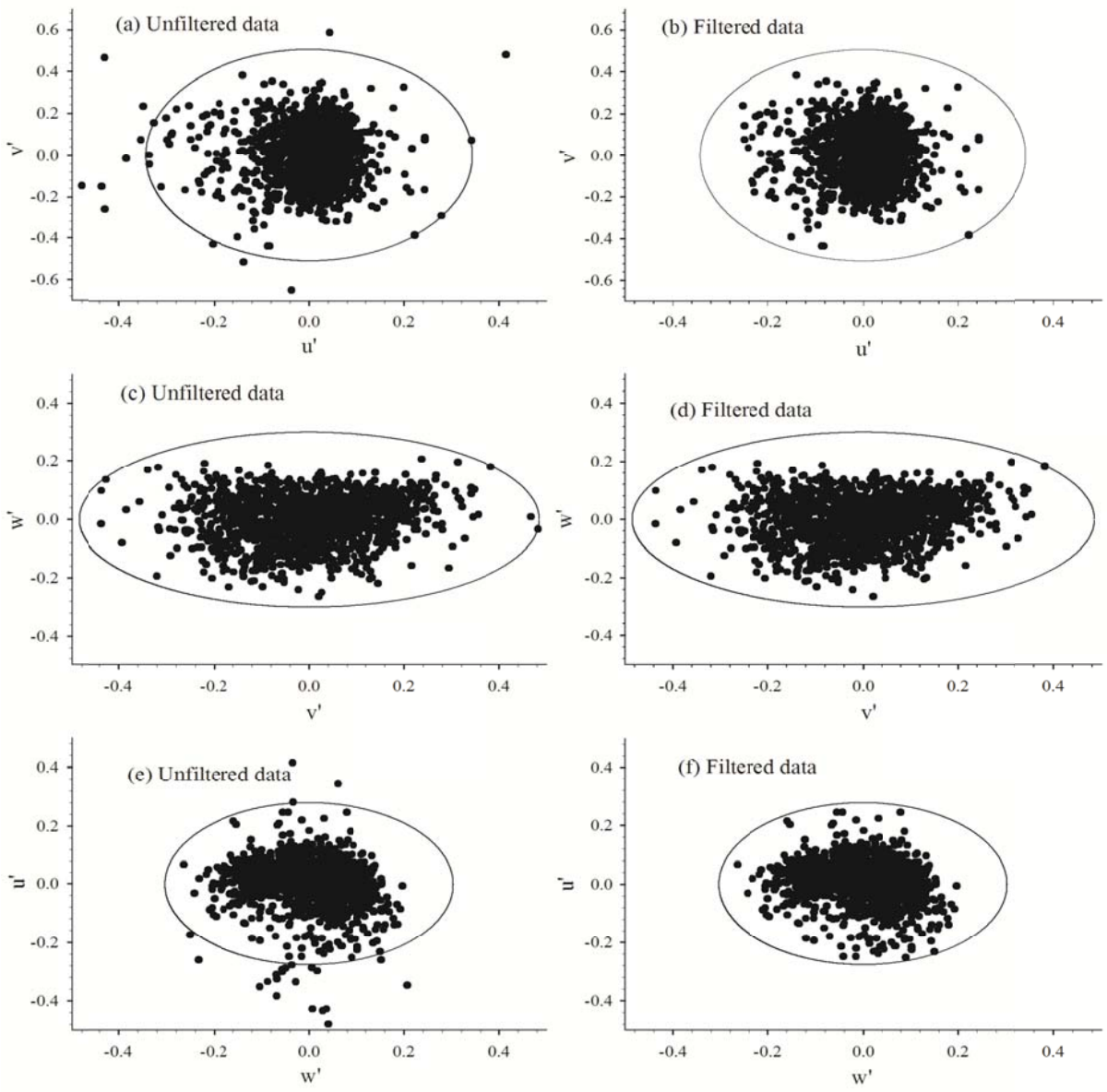

Fig. 4 Velocity correlation diagram of unfiltered and filtered data for (a) Unfiltered *u*'-*v*'; (b) Filtered *u*'-*v*'; (c) Unfiltered *v*'-*w*'; (d) Filtered *v*'-*w*;' (e) Unfiltered *w*'-*u*'; and (f) Filtered *w*'-*u*'

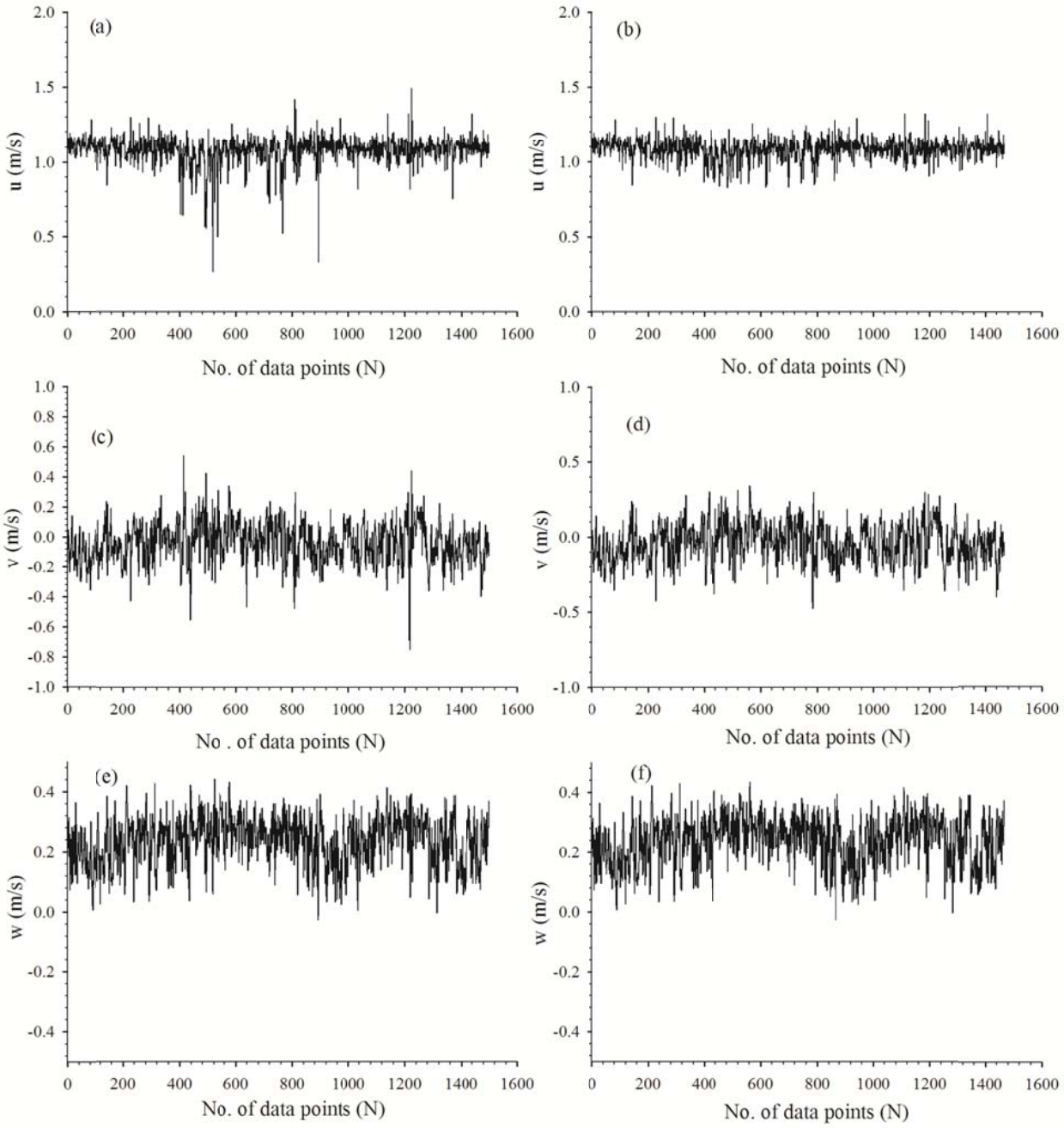

Fig. 5 Variation of velocity before and after filtering (a) Unfiltered *u*; (b) Filtered *u*; (c) Unfiltered *v*; d) Filtered *v*; e) Unfiltered *w*; f) Filtered *w*

C. *Turbulence Intensity Distribution*

Turbulence intensities of velocities in *x*, *y* and *z*-directions can be expressed as:

$$TI_u = \sqrt{\overline{u'^2}} / u_* \; ; TI_v = \sqrt{\overline{v'^2}} / u_* \; ; TI_w = \sqrt{\overline{w'^2}} / u_* \qquad (11a\text{-}c)$$

Here u', v' and w' are fluctuations in velocities in the directions *x*, y, and *z*, respectively; and u_* is the shear velocity. Variation of turbulence intensities along the longitudinal direction is shown in Fig. 6. The longitudinal turbulence intensity, TI_u, was found to increase along the length and after a certain distance it becomes constant. The increase in the turbulence intensity could be attributed to the development of boundary layer. At the leading edge of the block ramp, the thickness of boundary layer was thin and generation of turbulence was confined within it. However, as the boundary layer thickness increases downstream, the thickness of turbulence generated by bed would also increases. Thus the turbulence intensity would increase in downstream. However, when the boundary layer is fully developed i.e., increased up to the depth of flow, the turbulence intensity approaches a constant value. Similar results were obtained by Balachandar and Patel (2002) who studied the development of boundary layer on roughened flat plate.

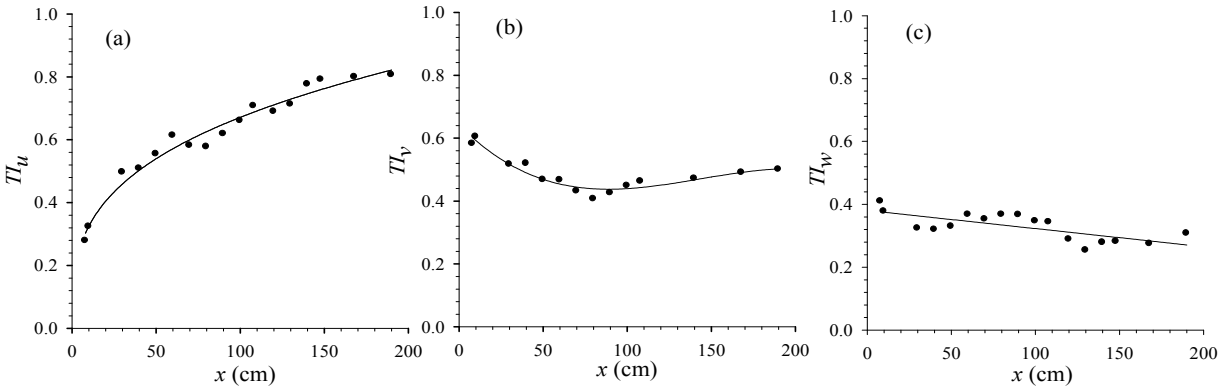

Fig. 6 Variation of (a) TI_u; (b) TI_v; and (c) TI_w along block ramp

Figure 6b shows that the transverse turbulent intensity, TI_v, decreases downstream and attains a constant value after a certain distance. The roughness elements act as obstruction to flow, which shred down large vortices and creates a transverse vortex sheet flow (Tritico and Hotchkiss 2005). This helps the transverse Reynolds stress component ($\overline{u'v'}$) to overtake the vertical Reynolds stress component ($\overline{u'w'}$) which signifies that the presence of obstruction enhances the transverse turbulence in form of wake of vortex sheet and inhibits the vertical turbulence. However, due to the interaction of wake generated by nearby roughness elements, the further production of turbulence in form of wake declines transverse turbulent intensities as shown in Fig. 6b. But as the boundary layer develops further downstream; the turbulence intensity approaches a constant value. This complies the finding of Balchandar and Patel (2002).

Vertical turbulence intensity, TI_w, decreases gradually downstream. This could be due to the breaking of large eddies into smaller eddies by the blocks (Tritico and Hotchkiss. 2005). Also the Grass (1971) has reinstated the fact of reverse correlation between vertical and longitudinal turbulent intensities. Therefore, this breaking of larger eddies into smaller eddies damps the magnitude of TI_w along the block ramp length.

D. Reynolds Stress Distribution

Previous studies indicate decrease in Reynolds stress from bed to water surface (Nezu and Rodi, 1986; Grass 1971; Bigillon et al., 2006). However, no information is available for variation of Reynolds stress in the direction of flow. Present study reveals that Reynolds stresses in all the three planes increase downstream due to the development of boundary layer over the block ramp (Figs. 7a, b, and c). Reynolds stress $\overline{u'v'}$ in *x-y* plane increases up to a peak and then tends to attain a constant value which is in accordance with the observations of Tritico and Hotchkiss (2005) and Shamloo et al. (2001). Similar trend was observed for Reynolds stress $\overline{u'w'}$ in *x-z* plane which was due to the de-attachment of shear layer due to the presence of large roughness elements (ejections) giving rise to increment in vertical Reynolds stress component. This finding complies with the observations of Lacey and Roy (2008), Papanicolaou et al. (2002), Nezu and Nakagawa (1993), Nakagawa and Nezu (1977), Raupach (1981).The Reynolds stress $\overline{v'w'}$ in *y-z* plane also increases linearly downstream as shown in Fig. 7c.

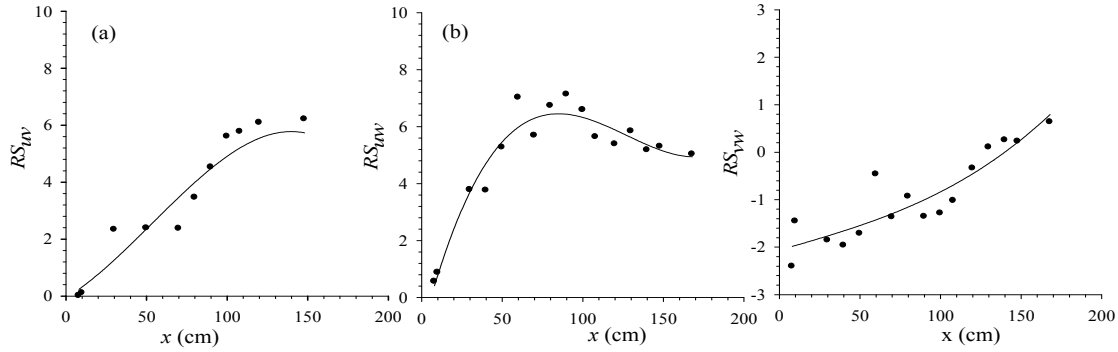

Fig. 7 Variation of Reynolds stress (a) $RS_{uv}=\overline{u'v'}$; (b) $RS_{uw}=\overline{u'w'}$; and (c) $RS_{vw}=\overline{v'w'}$ along the block ramp

E. Turbulent Kinetic Energy

The turbulent kinetic energy of turbulence is expressed as

$$TKE = \left(\overline{u'^2} + \overline{v'^2} + \overline{w'^2}\right)/2 \tag{12}$$

Turbulent kinetic energy decreases exponentially along the vertical direction and follows the following formula (Nezu and Nakagawa, 1993)

$$TKE/u_*^2 = 4.78\exp(-2z/h) \tag{13}$$

Present study indicates increase of turbulent kinetic energy downstream of the block ramp due to the development of boundary layer and due to excessive ejections of shed vortices from the roughness lying on the bed of the block ramp. This is in accordance with the observation of Nezu and Nakgawa (1993).Similar facts were also proved by Nakagawa and Nezu (1977) and Raupach (1981), who suggested that due to the presence of intermittent events of bursting mainly comprising of ejections and sweeps, the turbulent kinetic energy is transported over the flow domain. The spatial variation of turbulent kinetic energy is shown in Fig. 8.

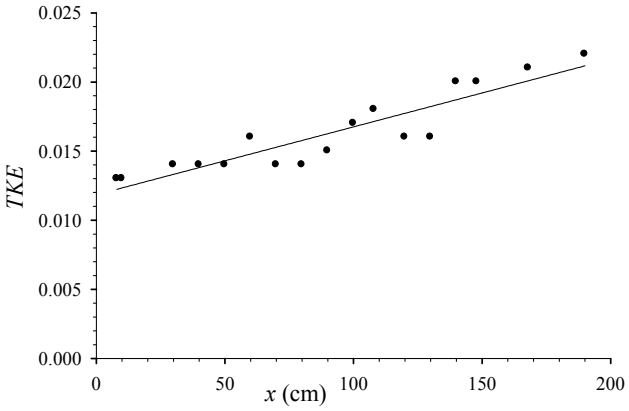

Fig. 8 Variation of turbulent kinetic energy along block ramp

F. Skewness Coefficients of Velocities

Skewness is defined as the factor or property of any random variable describing asymmetry of random variable about its mean. Mathematically

$$SK_u = \sum_{i=1}^{N} u'^3 \Big/ \left(N\left(\overline{u'^2}\right)^{3/2} \right) \tag{14}$$

The turbulence skewness factors represent the transporting parameters of turbulence energy due to the turbulence fluctuation in their respective directions. Spatial variation of coefficient of skewness of fluctuation in the velocity u, v and w are shown in Figs. 9a, b, c, respectively. Coefficient of skewness of u' and v' show random trend along the block ramp, however coefficient of skewness of w' increases from negative value to the positive value downstream of the block ramp as shown in Fig. 9c. Previous studies on turbulence near the bed explain negative skewness as ejection phase and positive skewness as the sweep phase of bursting phenomenon(Nikora and Smart, 1997; Bigillon et al., 2006; Agnelinchaab and Tachie, 2006; Balachandar and Bhuiyan, 2007; Lin et al., 2008).Increase in coefficient of skewness of w' is due to ejection and sweep phenomenon of the flow. At the beginning of block ramp, the shear layer starts de-attaching from the bed due to roughness effect. This results in retardation in fluid velocity which gives rise to ejections. Along the length as boundary layer grows and within the boundary layer the fluid rushes towards the bed to lift up the decelerated fluid lying between interstices of roughness on the bed and hence gives rise to the sweep phase of bursting. The predominance of sweeps and ejections in skimming flow is in accordance with the observations of Papanicolaou et al. (2001).Similar observations were noticed by many investigators like Nakagawa and Nezu (1977), Raupach (1981), Nezu and Nakagawa (1993), Balachandar and Bhuyian (2007).

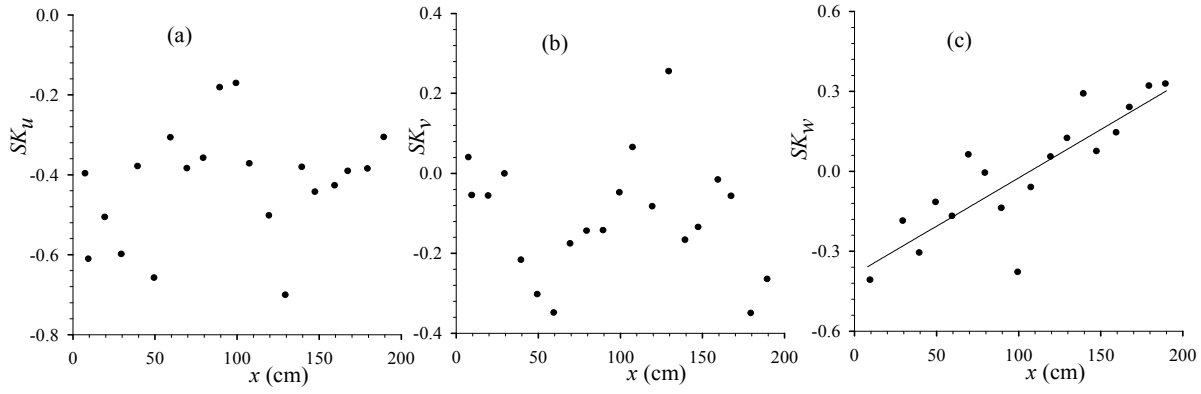

Fig. 9 Variation of coefficient of skewness of (a) u'; (b) v'; and (c) w' along block ramp

V. CONCLUSIONS

Various methods for filtering were studied in the present paper and out of the various methods, velocity correlation method was observed to be most suitable for the low correlation highly spiked ADV data. Study of turbulence in the developing of flow over a block ramp reveals that the turbulent intensity, u' increases along the ramp while transverse turbulent intensity, v' first decreases and then attains an equilibrium value. The vertical turbulence intensity, w', decreases along the block ramp due to breaking of larger eddies by the protrusions on the bed. Reynolds stress components $\overline{u'v'}$ and $\overline{u'w'}$ increase first and then attain an equilibrium value, whereas $\overline{v'w'}$ increases linearly along the block ramp. Turbulent kinetic energy increases along the length of block ramp. Skewness coefficients for u' and v' were uncorrelated with the block ramp length while skewness coefficients for w' increase linearly along the length of block ramps. Increase in coefficient of skewness of w' is due to ejection and sweep phenomenon of the bursting.

ACKNOWLEDGEMENTS

The first author would like to thank Mr. G. Schmid and supporting staff of Hydraulics Laboratory of Institute of Hydraulic Engineering, University of Stuttgart, Stuttgart, for their kind support during experimental work. Financial support from DAAD for visiting the first author to the University of Stuttgart is also greatly acknowledged.

NOMENCLATURE

a, b = Major and minor axes of threshold ellipsoid, respectively

a_i = Acceleration in i^{th} time interval

g = Acceleration due to gravity

h = Depth of flow

k_σ = Proportionality parameter in acceleration threshold method

m = slope of least squared fitted line in velocity correlation method

N = Number of data points

Sk_u = Skewness coefficient of u-component

Sk_v = Skewness coefficient of v-component

Sk_w = Skewness coefficient of w-component

$TI_u = \sqrt{\overline{u'^2}} \Big/ u_*$ = Relative turbulence intensity in x- direction

$TI_v = \sqrt{\overline{v'^2}} \Big/ u_*$ = Relative turbulence intensity in y- direction

$TI_w = \sqrt{\overline{w'^2}} \Big/ u_*$ = Relative turbulence intensity in z- direction

TKE = Turbulent kinetic energy

$\overline{u}$ = Temporally averaged velocity in x-direction

u_i = x- direction velocity component in i^{th}

u_{max} = Maximum threshold velocity for x- direction velocity component

u_{min} = Minimum threshold velocity for x- direction velocity component

u_* = Shear velocity

u' ,v', w'= Velocity fluctuations in x, y and z-directions, respectively

$\overline{u'v'}$ = Reynolds stress component in x-y plane

$\overline{u'w'}$ = Reynolds stress component in x-z plane

$\overline{v'w'}$ = Reynolds stress component in y-z plane

x, y, z = Longitudinal, transverse and vertical axes, respectively

Greek letters

Δu_i = First differentiation of i^{th} velocity component

$\Delta^2 u_i$ = Second differentiation of i^{th} velocity component

$\lambda = \sqrt{2\ln(N)}$ = Universal threshold parameter

λ_a= Proportionality constant

σ_{ax} = Standard deviation of acceleration component in x-direction

σ_{ay} = Standard deviation of acceleration component in y-direction

σ_{az} = Standard deviation of acceleration component in z-direction

σ_u = Standard deviation of u

$\sigma_{\Delta u}$ = Standard deviation of Δu

$\sigma_{\Delta^2 u}$ = Standard deviation of $\Delta^2 u$

θ = Angle of rotation of threshold ellipsoidal axes with reference axes

REFERENCES

[1] Agnelinchaab M, Tachie MF (2006) Open channel turbulent flow over hemispherical ribs. Int J of Heat and Fluid Flow 27: 1010-1027.

[2] Ahmad Z, Petappa NM, Westrich B (2009) Energy dissipation on block ramps with staggered boulders. J Hydraulic Eng 135(6): 522-526.

[3] Balachandar R, Bhuyian F (2007) Higher-order moments of velocity fluctuations in an open channel flow with large bottom roughness. J Hydraulic Eng 133(1): 77-87.

[4] Balachandar R, Patel VC (2002) Rough wall boundary layer on plates in open channel. J Hydraulic Eng 128 (10): 947-951.

[5] Bigillon F, Nino Y, Garcia MH (2006) Measurements of turbulence characteristics in an open channel flow over a transitionally rough bed using particle image Velocimetry. Exp Fluids 41: 857-867.

[6] Blinco PH, Partheniades E (1971) Turbulence characteristics in free surface flows over smooth and rough boundaries. J Hydraulic Res 9: 43-69.

[7] Carollo FG, Ferro V, Termini D (2005) Analyzing turbulence intensity in gravel bed channels. J Hydraulic Eng 131(12): 89-98.

[8] Cea L, Puertas J, Pena L (2007) Velocity measurements on highly turbulent free surface flow using ADV. Exp Fluids 42: 333-348.

[9] Chen X, Chiew YM (2003) Response of velocity and turbulence to sudden change of bed roughness in open channel flow. Journal Hydraulic Eng 129(1): 35-43.

[10] Ghare AD, Ingle RN, Porey PD, Gokhale SS (2010) Block ramp design for efficient energy dissipation. J Hydraulic Eng 136(3): 1-5.

[11] Goring DG, Nikora VI (2002) Despiking acoustic Doppler velocimeter data. J Hydraulic Eng 128(1): 117-126.

[12] Grass AJ (1971) Structural features of turbulent flow over smooth and rough boundaries. J Fluid Mechanics 50: 233-255.

[13] Lacey RWJ, Roy AJ (2008) The spatial characterization of turbulence around large roughness elements in a gravel-bed river. Geomorphology 102: 542-553.

[14] Lin J, Foucaut JM, Laval JP, Perenne N, Stansilas M (2008) Assessment of different SPIV processing methods for application to near wall turbulence. Applied Physics 112: 191-221.

[15] Nakagawa H, Nezu I (1977) Prediction of the contributions to the Reynolds stress from bursting events in open channel flows. J Fluid Mech. 80: 99-128.

[16] NezuI, Rodi W (1986) Open channel flow measurements with a laser Doppler anemometer. J Hydraulic Eng 112(5): 335-355.

[17] Nezu I, Nakagawa H (1993) Turbulence in open channel flows. Balkema Rotterdam The Netherlands.

[18] Nikora VI, Smart GM (1997) Turbulence characteristics of New Zealand gravel-bed rivers. J Hydraulic Eng 123(9): 764-773.

[19] Pagliara S, Chiavaccini P (2006) Energy dissipation on block ramps. J Hydraulic Eng 132(1): 41-48.

[20] Pagliara S, Chiavaccini P (2006) Energy dissipation on reinforced block ramps. J Irrigation Drainage Eng 132(3): 293-297.

[21] Pagliara S, Das R, Palermo M (2008) Energy dissipation on submerged block ramps. J Irrigation Drainage Eng 134(4): 527-532.

[22] Pagliara S, Lotti I (2009) Surface and subsurface flow through block ramps. J Irrigation Drainage Eng 135(3): 366-374.

[23] Papanicolaou AN, Diplas P, Dancey CL, Balakrishnan M (2001) Surface roughness effects in near bed turbulence implications to sediment entrainment. J Engineering Mechanics 127(2): 211-218.

[24] Raupach MR (1981) Conditional statistics of Reynolds stress in rough wall and smooth-wall turbulent boundary layers. J Fluid Mech. 108: 363-382.

[25] Shamloo H, Rajaratnam N, Katopodis C (2001) Hydraulics of simple habitat structures. J Hydraulic Res. 39(4): 351-366.

[26] Tritico HM, Hotchkiss RH (2005) Unobstructed and obstructed turbulent flow in gravel bed rivers. J Hydraulic Eng 131(8): 635-645.

[27] Wahl TL (2003) Discussion of despiking of acoustic Doppler velocimeter data. J Hydraulic Eng 129(6): 484-487.

[28] Wang J, Dong Z, Chen C, Xia Z (1993) The effects of bed roughness on the distribution of turbulent intensities in open channel flow. J Hydraulic Res 31(1): 89-98.